ANALYTICAL SCIENCES AUGUST 2001, VOL. 17



Reviews

# Dynamic Study of Metal-Ion Incorporation into Porphyrins Based on the Dynamic Characterization of Metal Ions and on Sitting-Atop Complex Formation

**Shigenobu FUNAHASHI,*† Yasuhiro INADA,** and Masahiko INAMO*****

**Laboratory of Analytical Chemistry, Graduate School of Science, Nagoya University, Chikusa, Nagoya 464–8602, Japan*
***Research Center for Materials Science, Nagoya University, Chikusa, Nagoya 464–8602, Japan*
****Department of Chemistry, Aichi University of Education, Igaya, Kariya, Aichi 448–8542, Japan*

We succeeded in the detection of the sitting-atop (SAT) copper(II) complex of TPP (5,10,15,20-tetraphenylporphyrin) in acetonitrile (AN) as a solvent with a very low Brønsted basicity, where two pyrrolenine nitrogens in the Cu(II)-SAT complex coordinate to the metal ion and two protons still remain on the pyrrole nitrogens. The structure parameters around the copper(II) ion in the Cu(II)-SAT complex, as determined by a fluorescent EXAFS method, suggest an axially elongated and equatorially distorted six-coordinate geometry. We measured the rates of the formation reaction of the SAT complexes for a series of transition metal(II) ions in AN using the stopped-flow technique. We propose the mechanism where there is a rapid deformation equilibrium of the porphyrin ring prior to the rate-determining step of the bond rupture of a coordinated solvent molecule on the metal(II) ion. Furthermore, we measured the rates of the deprotonation reaction of the Cu(II)-SAT complex by some Brønsted bases and indicated that the rate-determining step is the attack of the base on the proton of the pyrrole nitrogen in the SAT complex. Finally, a unified mechanism relevant to the porphyrin metalation mechanism has been proposed.

**(Received May 9, 2001; Accepted June 26, 2001)**



## 1 Introduction

The metalloporphyrin formation reaction is one of the important processes from both analytical and bioinorganic points of view. The large molar absorption coefficient and very high stability of the metalloporphyrins are very useful for the highly sensitive analysis of trace amounts of metal ions, and the size selectivity of the porphyrins is valuable for the separation of various kinds of metal ions.[1–7] A variety of metalloporphyrin formation rates are also applicable for the kinetic analysis of metal ions.[8,9] On the other hand, kinetic studies of metalloporphyrin formation are indispensable in order to understand *in vivo* metal

† To whom correspondence should be addressed.
E-mail: sfuna@chem4.chem.nagoya-u.ac.jp

incorporation processes leading to the natural metalloporphyrins. Generally porphyrins are synthesized in a metal-free form and metal ions are subsequently inserted. The latter process is catalyzed by enzymes, and a model for the catalytic function of the enzyme has been proposed as the porphyrin distortion caused by steric and electronic interactions with amino acid residues at the enzyme active site.[10-16] For example, the metalloporphyrin formation is a key reaction of the biosynthesis of heme, since the final step of the biosynthesis is the Fe(II) ion incorporation *in vivo* into the protoporphyrin IX.[17-20] For an understanding of the metalloporphyrin formation mechanism and the role of the enzymatic catalysis, further kinetic studies of the metalation have been required. In this context, the kinetics of the metalloporphyrin formation have been extensively studied for many kinds of metal ions in a variety of solvents in order to clarify the metalation mechansim of porphyrins.[21-30]

When the metal ion ($M^{n+}$) is incorporated into the porphyrin ($H_2$por) to form the metalloporphyrin ($M(por)^{(n-2)+}$), two amine protons in $H_2$por are dissociated from the two pyrrole groups as in Eq. (1).

$$M^{n+} + H_2por \rightleftharpoons M(por)^{(n-2)+} + 2H^+ \quad (1)$$

Because the two pyrrolenine groups can potentially bind to the metal ion, the overall metalation reaction will consist of at least two steps, *i.e.*, the coordination step of two pyrrolenine nitrogens to form an intermediate, the so-called sitting-atop (SAT) complex, $M(H_2por)^{n+}$,[31] in which two protons on the pyrrole nitrogens still remain,[32-35] and the deprotonation step of the SAT complex to form the metalloporphyrin, as shown by Eqs. (2) and (3), respectively.

$$M^{n+} + H_2por \rightleftharpoons M(H_2por)^{n+} \quad (2)$$

$$M(H_2por)^{n+} \rightleftharpoons M(por)^{(n-2)+} + 2H^+ \quad (3)$$

The separate observations of these two steps and their individual kinetic measurements are necessary to analyze the detailed mechanism of the overall metalation of the porphyrins. In order to separate these two steps, acetonitrile (AN) was selected as a solvent with a very low Brønsted basicity. In such a solvent, the released protons due to deprotonation of the SAT complex can not be thermodynamically stabilized according to Eq. (3). Furthermore, as expected from Eq. (2), the SAT complex can be much more stabilized in AN with its lower solvating ability than in strongly coordinating solvents such as *N*,*N*-dimethylformamide (DMF) and dimethyl sulfoxide (DMSO). As a result, we succeeded in the direct detection of the SAT complex of 5,10,15,20-tetraphenylporphyrin ($H_2$tpp) with the Cu(II) ion by the strategic use of AN as the solvent.[36] By structural characterization of the Cu(II)-SAT complex in AN by the $^1$H NMR and EXAFS methods, it was clarified that two pyrrolenine nitrogens coordinate to the equatorial sites of the Cu(II) ion and that $H_2$tpp acts as a bidentate ligand.[36,37] Furthermore, the SAT complex formation rates for the first-row transition metal(II) ions were demonstrated to be parallel to the rates for solvent exchange on the corresponding metal(II) ions.[37]

In addition, we recently carried out the kinetic measurements of the deprotonation of the Cu(II)-SAT complex of $H_2$tpp with a series of Brønsted bases, such as 3-methylpyridine (mpy), pyridine (py), dmso, and dmf and clarified the deprotonation mechanism.[38] Finally, we can propose the mechanism for the overall metalation of porphyrins. The structures of the porphyrins cited in this paper are shown in Scheme 1.

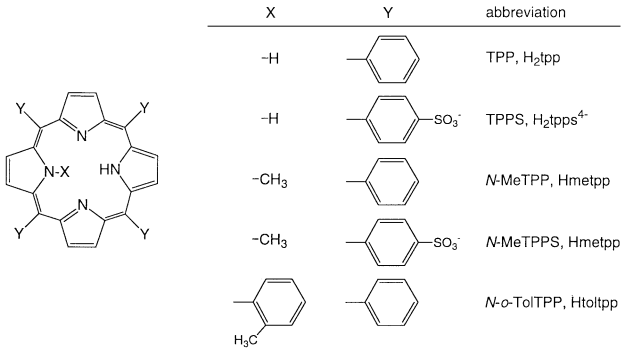


Scheme 1

## 2 Rates of Metalloporphyrin Formation Reaction

### 2·1 Metalloporphyrin formation relative to solvent exchange and complexation of metal ions

First, we will point out the metalloporphyrin formation reaction relative to the metal complex formation reaction and solvent exchange reaction. The metalloporphyrin formation of metal ions with porphyrins as a ligand is one of the complexation reactions. The Eigen mechanism is generally accepted for the complexation reactions (Eq. (4)) of many metal ions ($M^{n+}$) with conventional ligands ($L^{m-}$).[39-41] The Eigen mechanism involves the following processes. An outer-sphere complex, $M^{n+}\cdots L^{m-}$, between a metal ion and a ligand is formed with the association constant of $K_{os}$ due to electrostatic interaction, which is as fast as diffusion-control (Eq. (5)). The rate-determining step with the first-order rate constant of $k_i$ for the complexation is the dissociation of a directly coordinated solvent molecule in the inner-sphere of the metal ion (Eq. (6)). Therefore, the overall second-order rate constant, $k_f$, for complexation is given by the product of $K_{os}$ and $k_i$. This $k_i$ is almost equivalent to the rate constant ($k_{ex}$) for the solvent exchange on the respective metal ion. In fact, it has been confirmed that this is the case for many reaction systems.[40]

$$M^{n+} + L^{m-} \underset{}{\overset{k_f}{\rightleftharpoons}} ML^{(n-m)+} \quad (4)$$

$$M^{n+} + L^{m} \overset{K_{os}}{\rightleftharpoons} M^{n+}\cdots L^{m-} \quad (5)$$

$$M^{n+}\cdots L^{m-} \overset{k_i}{\rightleftharpoons} ML^{(n-m)+} \quad (6)$$

Interestingly, the rates of the complexation of porphyrins are much slower, by several orders of magnitude, than those of the acyclic ligands.[8,26,28] Such extraordinarily slow rates have been discussed in terms of the rigidity of the planar porphyrin framework. Meanwhile, for the *N*-substituted porphyrins, in which one of the two hydrogen atoms bound to the pyrrole nitrogen atoms is substituted by an alkyl or aryl group, displacement of the substituent from the porphyrin plane due to its bulkiness causes a tilting distortion of the pyrrole rings of the porhyrin. Lavallee's group and other groups investigated the kinetics of the complexation of the *N*-substituted porphyrins with several metal ions,[24,42-56] showing that the *N*-alkylporphyrins form metal complexes much faster than the corresponding non-*N*-alkylated porphyrins.[24,28,43]

### 2·2 Rates for metalation of TPP and *N*-substituted TPP in DMF

#### 2·2·1 Deformation effect of *N*-substituted TPP

For the *N*-substituted porphyrin, we will demonstrate the degree of deformation of the porphine ring and the effect of

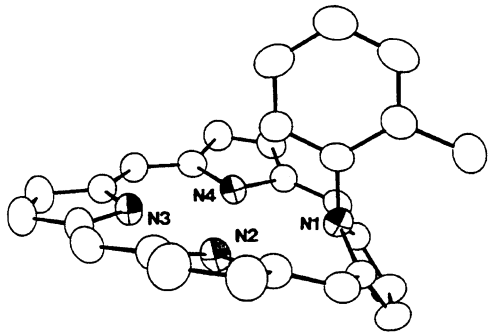


Fig. 1 Side-on view of the porphine core of *o*-TolTPP, with omission of the peripheral phenyl rings for clarity (adopted from Ref. 42 with permission).

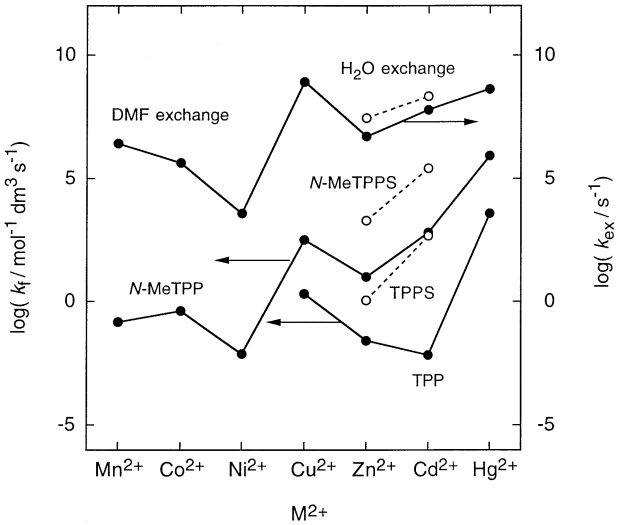


Fig. 2 Rate constants $k_f$ for metalation of *N*-MeTPP and TPP with divalent metal(II) ions ($M(dmf)_6^{2+}$) in DMF together with the rate constants $k_{ex}$ for solvent exchange on respective metal ions. The open circles for $Zn^{2+}$ and $Cd^{2+}$ ions are the corresponding rate constants in water.

deformation on the rate. In order to evaluate the deformation effect, we synthesized the deformed *N*-substituted porphyrin by the addition of bulky groups, that is, phenyl, *p*-tolyl, and *o*-tolyl groups on the pyrrole nitrogen. Fortunately, we could obtain single crystals of free *o*-TolTPP for X-ray analysis. Figure 1 is the side-on view, emphasizing the distortion of the porphine core, with omission of the peripheral phenyl rings for clarity (Fig. 1).[42]

The *N*-substituted pyrrole ring forms the most highly canted plane from the N1–N2–N4 reference plane, with a dihedral angle of 57.3°. The two adjacent pyrrole rings (that is, the N2 and N4 pyrrole rings) are tilted in the direction opposite to that of the N1-pyrrole ring. The dihedral angles are 19.3 and 16.4° for the N2- and N4-pyrrole rings, respectively. The protonated N3-pyrrole ring opposite to the N1-pyrrole ring forms a plane almost coplanar with the reference plane. Consequently, the bulkier *N*-*o*-tolyl group compels the porphine ring system to be more distorted than the *N*-methyl group of *N*-MeTPPBr$_4$ with a dihedral angle of 28°.[57]

The rate for the incorporation reaction of Zn(II) ion into *o*-TolTPP and *N*-MeTPP in DMF solution is definitely second-order with respect to the porphyrin and the metal ion. The metalation rate for *o*-TolTPP with $k$ (25°C) = 35 mol$^{-1}$ kg s$^{-1}$ is faster than that for *N*-MeTPP with $k$ (25°C) = 10 mol$^{-1}$ kg s$^{-1}$.[42] Since the rapid deformation equilibrium of the porphine core precedes the rate-determining solvent loss,[24,28,29,43] the difference in rate between the metalloporphyrin formation for *o*-TolTPP and *N*-MeTPP reflects the difference in the degree of the deformation. The crystal structures show a more favorable distortion of *o*-TolTPP for the complexation compared to *N*-MeTPPBr$_4$,[57] which has basically the same *N*-methylporphine core as *N*-MeTPP, and the bulkiness of the *N*-substituent group enhances the reactivity.

### 2·2·2 Rates for metalation of TPP and *N*-MeTPP in DMF

We determined the second-order rate constants ($k_f$) for the metalation of *N*-MeTPP and TPP using a series of divalent metal(II) ions ($M^{2+}$) in *N*,*N*-dimethylformamide (DMF).[28,29,58] The logarithmic values of $k_f$ are plotted in Fig. 2 together with the first-order rate constants, $k_{ex}$, for solvent exchange on the respective metal ions in DMF. As is apparent from Fig. 2, the trend in the rate constant variation for a series of metal ions for the DMF solvent exchange and for the metalation of *N*-MeTPP and TPP in DMF is very similar, although there is a difference of several orders of magnitude for each series. In addition, the same trend is observed for the water exchange and metalation of *N*-MeTPPS and TPPS in water for zinc(II) and cadmium(II) ions.[6] Moreover, the rates decrease in the following order: solvent exchange, *N*-MeTPP metalation, and TPP metalation for the respective metal(II) ion. Thus the metalation rate for TPP is very much slower by several orders of magnitude than those for the complexation of normal ligands, and the metalation of *N*-methylated TPP is much faster than TPP. We can deduce the following three points. (a) The rate-determining step for the metalation of the porphyrin is the dissociation of a coordinated solvent molecule from the metal ion in the outer-sphere association complex (Eq. (9)). (b) Deformation of the porphine ring prior to the rate-determining step should be required (Eq. (7)). (c) Therefore, the overall rate constant ($k_f$) for the metalloporphyrin formation is given by the product of the equilibrium constant ($K_D$) for the deformation of the porphyrin ring, the equilibrium constant ($K_{os}$) for the outer-sphere complex formation, and the rate constant ($k_i$) for the dissociation of the coordinating solvent molecules in the inner-sphere of the metal(II) ions: $k_f = K_D K_{os} k_i$.

$$\mathrm{Hpor} \overset{K_D}{\rightleftharpoons} \mathrm{H}\textit{por} \quad (7)$$

$$\mathrm{M(dmf)_6^{2+}} + \mathrm{H}\textit{por} \overset{K_{os}}{\rightleftharpoons} \mathrm{M(dmf)_6^{2+}\cdots H}\textit{por} \quad (8)$$

$$\mathrm{M(dmf)_6^{2+}\cdots H}\textit{por} \overset{k_i}{\rightleftharpoons} \mathrm{M(por)} \quad (9)$$

where Hpor indicates $H_2$tpp, Hmetpp, $H_2$tpps$^{4-}$, and Hmetpps$^{4-}$, and H*por* is the deformed Hpor. Deformation of the porphyrin ring should be required for the metal ion to effectively interact with the nitrogen atom on the pyrrole group.

## 3 Formation and Demetalation of Metalloporphyrins in Aqueous Solution

### 3·1 Equilibria and kinetics of complexation of TPPS and *N*-MeTPPS with Cd(II) and Zn(II) ions in aqueous solution

Because it is difficult for us to determine the hydrogen ion dependency for the metalloporphyrin formation reactions in DMF as an aprotic solvent, we studied the water-soluble

metalloporphyrins in water in order to elucidate the hydrogen ion contribution to the mechanism. In this section, we describe the equilibria, kinetics and mechanisms of the complexation reactions of water-soluble *N*-MeTPPS and TPPS with cadmium(II) and zinc(II) ions in aqueous solution at various temperatures and pressures, as shown by Eqs. (10) and (11):[6]

$$\mathrm{Hmetpps^{4-} + M^{2+} \underset{k_d}{\overset{k_f}{\rightleftharpoons}} M(metpps)^{3-} + H^+} \quad (10)$$

$$\mathrm{H_2tpps^{4-} + M^{2+} \underset{k_d}{\overset{k_f}{\rightleftharpoons}} M(tpps)^{4-} + 2H^+} \quad (11)$$

where $Hmetpps^{4-}$ and $H_2tpps^{4-}$ are the free bases of *N*-MeTPPS and TPPS, and $k_f$ and $k_d$ are the rate constants for the formation and dissociation of the metalloporphyrin, respectively. The equilibrium constants for reactions (10) and (11) are defined as follows: $K_M^{N\text{-MeTPPS}} = [M(metpps)^{3-}][H^+][Hmetpps^{4-}]^{-1}[M^{2+}]^{-1}$ and $K_M^{TPPS} = [M(tpps)^{4-}][H^+]^2[H_2tpps^{4-}]^{-1}[M^{2+}]^{-1}$.

The interatomic distances between the metal ion and the oxygen atom of the coordinated water molecules in the aquated metal ion $[M(H_2O)_6]^{2+}$ have been determined by the EXAFS technique. The M-O distance is 2.27 Å for M = Cd(II) and 2.07 Å for M=Zn(II).[59] The cadmium(II) ion is not expected to fit well inside the central cavity of the porphyrin dianion, because the distance between the two nitrogen atoms on a diagonal of the porphyrin core is 4 Å. Such a difference in size of the $d^{10}$ Cd(II) and Zn(II) ions should be characteristic of the thermodynamic and kinetic behaviors as the metal ion size effect. Moreover, the methyl substituent at the pyrrole nitrogen in *N*-MeTPPS should cause steric hindrance for the metal ion incorporation even for the smaller Zn(II) ion as well as the porphyrin ring deformation.

### 3·1·1 Basicity of free porphyrin bases

The first and second protonation constants, $K_{H1}$ and $K_{H2}$, for $Hmetpps^{4-}$ and $H_2tpps^{4-}$ are as follows: log $K_{H1}$ and log $K_{H2}$ are 8.88 and 2.98 for *N*-MeTPPS[6] and 4.99 and 4.76 for TPPS,[60] respectively. Therefore, the free base of the *N*-substituted porphyrin is a much stronger base, by about 4 p*K* units, compared with the non-*N*-substituted porphyrin base. *N*-Monoalkylation of the porphyrins results in distortion of the porphine ring by an $sp^3$ hybridization of one of the pyrrolenic nitrogens; the substituted group is out-of-plane with respect to the three unsubstituted pyrrolenic nitrogens, as described in 2·2·1. Therefore, the bulky *N*-methyl group forces the porphyrin nucleus to distort from planarity as a deformation effect. Such a feature is reflected in the protonation constant.

## 3·2 Thermodynamic effects of porphyrin ring deformation and metal ion size

In Table 1 are tabulated the thermodynamic parameters for the metalloporphyrin formation of Cd(II) and Zn(II) ions with *N*-MeTPPS and TPPS in aqueous solution.[6]

For TPPS, the difference in the free energy change ($\Delta G^\circ$ at 25°C) for the metalloporphyrin formation between $Cd^{2+}$ and $Zn^{2+}$ is 51.4 kJ $mol^{-1}$, while for *N*-MeTPPS, it is 19.2 kJ $mol^{-1}$ (see Table 1). On the other hand, because the formation constants of $Cd^{2+}$ and $Zn^{2+}$ complexes of 2,2′-bipyridine (bpy) as an acyclic ligand are $10^{4.33}$ and $10^{5.23}$ $M^{-1}$ at 25°C, respectively,[61] the difference in $\Delta G^\circ$ is only 5 kJ $mol^{-1}$. With respect to the difference in the $\Delta G^\circ$ value between the two metal ions, the difference for *N*-MeTPPS is larger than that for an acyclic ligand of bpy, while the difference for TPPS is significantly large. This strongly indicates that the zinc(II) ion should be comfortably incorporated inside the porphyrin core of TPPS, but uncomfortable inside *N*-MeTPPS due to steric hindrance of the *N*-methyl group, while the cadmium(II) ion just sits on the porphyrin nucleus due to its size. This difference is also reflected in the kinetic parameters (*vide infra*). Although the complex formation reactions between the aquated metal ions with nitrogenous bases in aqueous solution are usually exothermic, the complexation reactions for the porphyrin ligands are endothermic (see Table 1). This comes from the inclusion of released pyrrolenic protons of the free base porphyrin in the metalloporphyrin formation as defined here.

Table 1 Thermodynamic parameters for metalloporphyrin formation of cadmium(II) and zinc(II) ions with *N*-MeTPPS and TPPS in aqueous solution at $I$ = 0.10 M

| | $Cd^{2+}$ | $Zn^{2+}$ |
|---|---|---|
| N-MeTPPS[a] | | |
| $K_M^{N\text{-MeTPPS}}$ (25.0°C) | $(1.16 \pm 0.03) \times 10^{-2}$ | $(2.87 \pm 0.18) \times 10$ |
| $\Delta G^\circ$/kJ $mol^{-1}$ (25.0°C) | 11.0 | –8.2 |
| $\Delta H^\circ$/kJ $mol^{-1}$ | 26.2 ± 2.0 | 34.6 ± 0.7 |
| $\Delta S^\circ$/$JK^{-1}$ $mol^{-1}$ | 51 ± 6 | 144 ± 3 |
| TPPS[b] | | |
| $K_M^{TPPS}$/M (25.0°C) | $1.15 \times 10^{-10}$ | $3.7 \times 10^{-1}$ |
| $\Delta G^\circ$/kJ $mol^{-1}$ (25.0°C) | 56.9 | 5.5 |
| $\Delta H^\circ$/kJ $mol^{-1}$ | 37.3[c] | 23.4[c] |
| $\Delta S^\circ$/$JK^{-1}$ $mol^{-1}$ | –66[c] | 60[c] |

a. $K_M^{N\text{-MeTPPS}} = [M(metpps)^{3-}][H^+][M^{2+}]^{-1}[Hmetpps^{4-}]^{-1}$.
b. $K_M^{TPPS} = [M(tpps)^{4-}][H^+]^2[M^{2+}]^{-1}[H_2tpps^{4-}]^{-1}$.
c. Estimated using the kinetic parameters listed in Table 2.

## 3·3 Kinetic effects of porphyrin ring deformation and metal ion size

In Table 2 are summarized the activation parameters for the formation and dissociation of metalloporphyrins of Cd(II) and Zn(II) ions with *N*-MeTPPS and TPPS.[6] The forward reaction is second order with respect to the metal ion and free base porphyrin. The reverse reaction is first order for the metalloporphyrin and second order for the hydrogen ion concentration in the case of TPPS, but first order for the hydrogen ion concentration in the case of *N*-MeTPPS. This finding indicates that the deprotonation of pyrrole protons for the forward reaction is not rate-determining and that the protonation on the pyrrole nitrogens for the reverse reaction is fast and not rate-determining.

One of the most characteristic features for the metalloporphyrin formation is the slowness of the rate in comparison with acyclic ligands. In the previous section, we demonstrated that the overall rates for the metalloporphyrin formation correlate with the rate of the solvent exchange reaction of the metal ions.[29] The interpretation was based on the multistep reaction mechanism including the following steps: (1) deformation of the porphyrin, (2) outer-sphere complex formation between the metal ion and the deformed porphyrin *via* electrostatic interaction, (3) solvent dissociation on the metal ion and bond formation between the metal ion and porphyrin donor atom, and (4) dissociation of the pyrrolenic protons. For the dissociation of the metalloporphyrins, the proton addition step is included, *i.e.*, the rate is first order for $M(metpps)^{3-}$ and second order for $M(tpps)^{2-}$ with respect to the hydrogen ion concentration, but the proton dissociation step is not included for the formation, because the formation rate is independent of the hydrogen ion concentration (*vide supra*). Thus, the second-order rate constant $k_f$ for the metalloporphyrin formation can be expressed as $k_f = K_D K_{OS} k_i$, where $K_D$, $K_{OS}$, and $k_i$ refer to the deformation equilibrium constant of the

Table 2 Activation parameters for formation and dissociation of metalloporphyrins of cadmium(II) and zinc(II) ions with *N*-MeTPPS and TPPS at $I$ = 0.10 M

| | $Cd^{2+}$ | $Zn^{2+}$ |
|---|---|---|
| *N*-MeTPP | | |
| $k_f$/$M^{-1}$ $s^{-1}$ (25.0°C) | $2.53 \times 10^5$ | $2.10 \times 10^3$ |
| $\Delta H_f^{\ddagger}$/kJ $mol^{-1}$ | 37.9 ± 1.0 | 54.6 ± 0.9 |
| $\Delta S_f^{\ddagger}$/J $mol^{-1}$ $K^{-1}$ | –15 ± 3 | 2 ± 3 |
| $\Delta V_f^{\ddagger}$/$cm^3$ $mol^{-1}$ | –1.0 ± 0.4 | 2.8 ± 0.9 |
| $k_d$/$M^{-1}$ $s^{-1}$ (25.0°C)[a] | $1.96 \times 10^7$ | $6.37 \times 10$ |
| $\Delta H_d^{\ddagger}$/kJ $mol^{-1}$ | 14.3 ± 0.8 | 19.3 ± 1.5 |
| $\Delta S_d^{\ddagger}$/J $mol^{-1}$ $K^{-1}$ | –57 ± 3 | –146 ± 5 |
| $\Delta V_d^{\ddagger}$/$cm^3$ $mol^{-1}$ | –9.6 ± 0.5 | |
| TPPS | | |
| $k_f$/$M^{-1}$ $s^{-1}$ (25.0°C) | $5.21 \times 10^2$ | 1.13 |
| $\Delta H_f^{\ddagger}$/kJ $mol^{-1}$ | 49.5 ± 3.1 | 57.8 ± 2.4 |
| $\Delta S_f^{\ddagger}$/J $mol^{-1}$ $K^{-1}$ | –27 ± 2 | –50 ± 3 |
| $\Delta V_f^{\ddagger}$/$cm^3$ $mol^{-1}$ | –6.4 ± 0.3 | 3.9 ± 0.3 |
| $k_d$/$M^{-2}$ $s^{-1}$ (25.0°C)[b] | $5.49 \times 10^{12}$ | 9.37 |
| $\Delta H_d^{\ddagger}$/kJ $mol^{-1}$ | 12.2 ± 1.5 | 34.4 ± 1.5 |
| $\Delta S_d^{\ddagger}$/J $mol^{-1}$ $K^{-1}$ | 39 ± 5 | –110 ± 3 |

a. Rate = $k_d$[M(metpps)$^{3-}$][$H^+$].
b. Rate = $k_d$[M(tpps)$^{4-}$][$H^+$]$^2$.

porphyrin, the equilibrium constant for the outer-sphere association, and the first-order rate constant for the interchange of a coordinated water molecule with a donor atom of the entering deformed porphyrin ligand.

The slowness is due to the energy required for the deformation corresponding to $K_D$. The deformation should be required for metal ions to interact with donor atoms of the porphyrin. As apparent from Table 2, the second-order rate constants for the complex formation reaction of *N*-MeTPPS are much larger than those of TPPS. The enhancement in rate amounts to 1900 times for Zn(II) and 480 times for Cd(II). Interestingly, the forward reaction for the metalloporphyrin formation is faster by about two orders of magnitude for Cd(II) than for Zn(II) for both *N*-MeTPPS and TPPS. The difference in rate reasonably corresponds to that in rate for the water exchange on the metal(II) ions. It was found that for *N*-methylporphyrin in DMF there is also a correlation between the complex formation rate and the solvent exchange rate of the metal ions.[29] Since the *N*-substituted porphyrin is deformed from the planar molecular structure of the porphyrin due to the steric bulkiness of the substituent, the $K_D$ value should be much larger for the *N*-substituted porphyrin than that for the non-*N*-substituted porphyrin. The enhancement in the rate indicates that the deformation for the metal ion accommodation is significantly established by the methylation. Consequently, these are the cases for the situation between TPP and *N*-MeTPP in DMF (see 2·2·2). It should be noted that the dissociation rates of the TPPS and *N*-MeTPPS complexes are second-order and first order with respect to the hydrogen ion concentration, respectively. This strongly indicates that the species of the porphyrins in the transiton state are free bases, *i.e.*, $H_2tpps^{4-}$ and $Hmetpps^{4-}$. The difference in the acid-catalyzed dissociation rate is significant, *i.e.*, the ratio of the rate constants between $Cd^{2+}$ and $Zn^{2+}$ is $3 \times 10^5$ for *N*-MeTPPS and $6 \times 10^{11}$ for TPPS (see Table 2).

The activation volume, $\Delta V^{\ddagger}$, for the complexation reaction is considered as a diagnostic of the reaction mechanism. The $\Delta V^{\ddagger}$ values for the complexation reaction of Zn(II) and Cd(II) ions with bpy in aqueous solution are $\Delta V^{\ddagger}$ = 7.4 ± 0.4 $cm^3$ $mol^{-1}$ for the Zn(II) ion and –5.5 ± 1.0 $cm^3$ $mol^{-1}$ for the Cd(II) ion.[61] The difference in the sign of the $\Delta V^{\ddagger}$ values was considered as the change in the activation mode from the dissociative interchange to the associative interchange going from the first to the second row, which is attributed to the large difference in ionic radius between the two metal ions. It is believed that the larger Cd(II) ion has enough room around itself to accommodate a seventh donor atom in the transition state. Interestingly, the same tendency in the $\Delta V^{\ddagger}$ values has been observed for the TPPS and *N*-MeTPPS systems, *i.e.*, the positive values of $\Delta V^{\ddagger}$ for $Zn^{2+}$ (2.8 ± 0.9 (*N*-MeTPPS) and 3.9 ± 0.3 (TPPS) $cm^3$ $mol^{-1}$) and the negative values of $\Delta V^{\ddagger}$ for $Cd^{2+}$ (–1.0 ± 0.4 (*N*-MeTPPS) and –6.4 ± 0.3 (TPPS) $cm^3$ $mol^{-1}$). For the multistep reaction mechanism for the metalloporphyrin formation: $k_f = K_D K_{OS} k$ (*vide supra*), the rate-determining step corresponds to the interchange of a coordinated water molecule on the metal(II) ion with a donor atom of the entering deformed porphyrin ligand. Since we can accept that the volume change for the deformation ($K_D$) and for the outer-sphere complex formation ($K_{OS}$) is negligible, the activation mode for the metalloporphyrin formation is consequently, associative-interchange for the Cd(II) ion and dissociative-interchange for the Zn(II) ion.

## 4 Metalloporphyrin Formation Catalyzed by Large Metal Ions

The metalation rates of the fourth-row metal(II) ions, such as Mn(II), Cu(II), and Zn(II) ions, are highly accelerated by the presence of a small amount of metal(II) ions having a larger ionic radius, such as Cd(II), Pb(II), and Hg(II) ions. This has been interpreted by the possibility that the fast coordination to a larger metal(II) ion leads to a distorted porphyrin skeleton that easily incorporates the smaller metal(II) ion into the porphyrin core. Using the acceleration effect of this reaction system, Tabata *et al.* proposed the catalytic determination method of ultratrace amounts of mercury.[9]

### 4·1 Dinuclear metalloporphyrin formation

Tabata and Hambright *et al.* obtained evidence for an intermediate heterodinuclear metalloporphyrin complex in which two different metal ions are simultaneously bound to a porphyrin on the opposite sides.[62,63] According to the kinetic investigation for the Cu(II) ion incorporation into TPPS in the presence of the Hg(II) ion in water, the heterodinuclear porphyrin complex, in which two different metal ions simultaneously bind to $tpps^{6-}$, was shown as the reaction intermediate in the Cu(II) ion incorporation process. Under the conditions $[Cu^{2+}] > [Hg^{2+}] >> [H_2tpps^{4-}]$, the processes for this reaction system in weakly acidic media are established as follows:

$$Hg_2(tpps)^{2-} \underset{k_{-1}}{\overset{k_1}{\rightleftharpoons}} Hg(tpps)^{4-} + Hg^{2+} \quad (12)$$

$$Hg(tpps)^{4-} + Cu^{2+} \xrightarrow{k_2} Hg(tpps)Cu^{2-} \quad (13)$$

$$Hg(tpps)Cu^{2-} \xrightarrow{k_3} Cu(tpps)^{4-} + Hg^{2+} \quad (14)$$

where $k_1 = 1.95 \times 10^8$ $s^{-1}$, $k_2/k_{-1} = 7.14$, and $k_3 = 1.00 \times 10^{-2}$ $s^{-1}$ at 25°C.[62] The reaction then proceeds with a two-stage kinetic behavior, and the first- and second-step reactions correspond to the formation of the heterodinuclear intermediate $Hg(tpps)Cu^{2-}$ and the final product $Cu(tpps)^{4-}$, respectively. Knowing the rate equation and the rate constants, we could set up the reaction conditions where almost all the copper ions exist as the

Table 3 Structure parameters around the Cu(II) ion in Cu(II)/Hg(II) heterodinuclear porphyrin intermediate

| Compound | Interaction[a] | $N$[b] | $R$[c]/pm |
|---|---|---|---|
| Intermediate | $Cu–N_{eq}$ | 2 | 204 ± 1 |
| | $Cu–O_{eq}$ | 2 | 195 ± 1 |
| | $Cu–O_{ax}$ | 2 | 238 ± 2 |
| $Cu(H_2O)_6^{2+}$ | $Cu–O_{eq}$ | 4 | 196 ± 1 |
| | $Cu–O_{ax}$ | 2 | 229 ± 3 |
| $Cu(tspp)^{4-}$ | Cu–N | 3.8 ± 0.2 | 200 ±1 |
| $Cu(py)_2(an)_4^{2+}$ [d] | $Cu–N(py)_{eq}$ | 2 | 202 |
| | $Cu–N(an)_{eq}$ | 2 | 202 |
| | $Cu–N(an)_{ax}$ | 2 | 230 |
| $Cu(en)(H_2O)_4^{2+}$ [e] | $Cu–N_{eq}$ | 2 | 200 |
| | $Cu–O_{eq}$ | 2 | 198 |
| | $Cu–O_{ax}$ | 2 | 231 |

a. The subscripts, "eq" and "ax", represent the equatorial and axial site of the Cu(II) center, respectively.
b. Coordination number.
c. Bond distance.
d. py = pyridine and an = acetonitrile, Ref. 36.
e. en = ethylenediamine, Ref. 67.

intermediate formed within 100 ms during the 10 s after mixing the mercury-porphyrin solution and the copper ion solution.

### 4·2 Structure determination of the short-lived intermediate formed during copper(II) ion incorporation into porphyrin using the stopped-flow EXAFS method

We developed a stopped-flow EXAFS apparatus (SF-EXAFS, Type FIT-6) by combining the stopped-flow and the EXAFS methods.[64,65] The time-resolved EXAFS measurement has been carried out in the vicinity of the Cu K edge for the Cu(II)/Hg(II) heterodinuclear porphyrin intermediate. We could measure the EXAFS spectra of copper in the intermediate for 10 s in one run. Thus EXAFS measurements were repeated 180 times to accumulate the EXAFS data to obtain a good EXAFS spectra. We determined the structure parameters around the Cu(II) ion in the Cu(II)/Hg(II) heterodinuclear porphyrin intermediate, which are summarized in Table 3 along with those of some relative copper(II) complexes.[66]

The $Cu–N_{eq}$ bond length of the Cu(II)/Hg(II) heterodinuclear porphyrin intermediate is similar to the $Cu–N(py)_{eq}$ bond length of the $[Cu(py)_2(an)_4]^{2+}$ complex (py = pyridine and an = acetonitrile),[36] where two py molecules, which have an $sp^2$-hybrid nitrogen equal with the pyrrolenine nitrogens of $tpps^{6-}$, coordinate to the Cu(II) ion in the *cis* position. Furthermore, the $Cu–O_{eq}$ and $Cu–O_{ax}$ bond lengths of the intermediate are respectively similar to the corresponding bond lengths in the $[Cu(en)(H_2O)_4]^{2+}$ complex (en = ethylenediamine).[67] These similarities in the bond lengths between the intermediate and the stable Cu(II) complexes indicate that the heterodinuclear intermediate is a metastable state in the Cu(II) ion incorporation process in the presence of the Hg(II) ion. The $Cu–N_{eq}$ bond length in the intermediate is thus longer than that of the most stable state in the system, $[Cu(tpps)]^{4-}$ complex, in which the Cu(II) ion is highly packed within the tetragonal porphyrin core of $tpps^{6-}$. These structural results indicate that the porphyrin skeleton in the Cu(II)/Hg(II) heterodinuclear porphyrin intermediate is distorted in the saddle-type as shown in Fig. 3, where the geometry around the Cu(II) center is a distorted octahedral and the two pyrrolenine nitrogens of $tpps^{4-}$ coordinate at the equatorial sites of the Cu(II) ion with a *cis* geometry.[66,68]

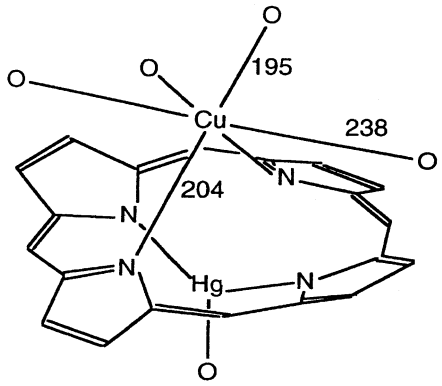


Fig. 3 Structure of the Cu(II)/Hg(II) heterodinuclear porphyrin intermediate. 4-Sulfonatophenyl groups are omitted. The structure around the Hg(II) ion is estimated on the basis of the structure parameters for $Hg_2(tpps)^{2-}$.[68]

## 5 Kinetics and Mechanism for Sitting-Atop (SAT) Complex Formation

In 1960, Fleischer and Wang first proposed the so-called sitting-atop complexes of the protoporphyrin dimethyl ester in chloroform on the basis of visible spectra, infrared spectra, and composition of the SAT complex.[31] After this report, the reports on the detection of the SAT complex have been very limited, only in peculiar systems.[32-35] We think that a crucial point to form the SAT complex is to guarantee the thermodynamic and kinetic retardation of the dissociation of protons on the pyrrole rings in the SAT complex. Therefore, we must select solvents with a very low Brønsted basicity; water as a solvent is not adequate. Acetonitrile (AN) has a very low Brønsted basicity and is a coordinating and aprotic solvent with a considerably high dielectric constant of 36, which is favorable for coordination ability and solubility.

### 5·1 Characterization of the SAT complex of Cu(II) ion based on the electronic and NMR spectra

Figure 4A shows the spectral change for the reaction between $Cu^{2+}$ and $H_2tpp$ in AN.[36] This process was completed within *ca.* 100 ms even in an excess $Cu^{2+}$ concentration on the order of $10^{-4}$ mol $dm^{-3}$. This reaction was extremely fast in comparison with the usual metalloporphyrin formation of the Cu(II) ion and was extremely slow compared with the normal complexation reaction of the Cu(II) ion. The absorption spectrum of the product (max = 406 nm) is apparently different from those of $H_2tpp$ (max = 417 nm) and Cu(tpp) (max = 414 nm) and has a characteristic broader Soret band compared with those of $H_2tpp$ and Cu(tpp) which have good symmetry in structure. These findings suggest that the porphyrin ring in the product should be distorted.

Figure 4B shows the $^1H$ NMR peaks assigned to the N–H and $\beta$-pyrrole protons for $H_2tpp$ in $CDCl_3$ and the Cu(II)-SAT complex in $CD_3CN$. The finding that the signal of the N–H protons in the Cu(II)-SAT complex was clearly observed at –2.05 ppm strongly indicated that the N–H protons remain in the SAT complex ($Cu(H_2tpp)^{2+}$). In contrast to the case of $H_2tpp$, two kinds of $\beta$-protons for the SAT complex were observed with a ratio of 1:1, which had twice the area of the peak for the NH protons. The peaks, one a singlet and the other a doublet, were attributed to the protons in the pyrrolenine groups coordinated to the Cu(II) ion and in the pyrrole groups not

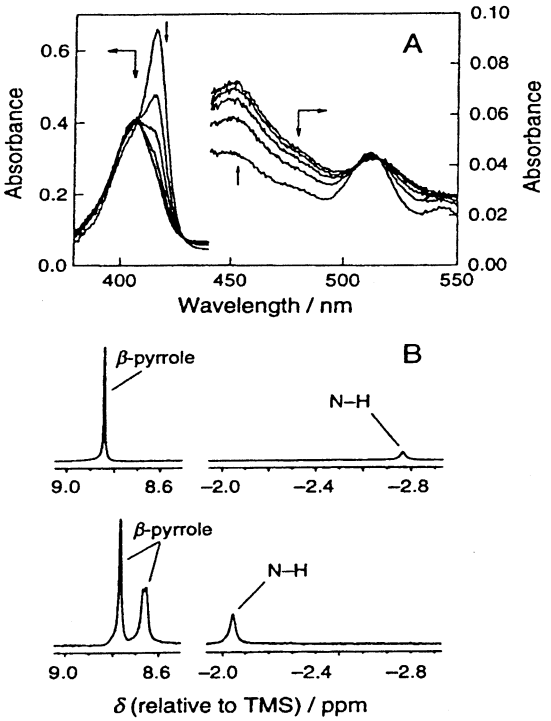


Fig. 4 Spectral change for the formation of the SAT complex (A) and $^1$H NMR spectra for $H_2$tpp and the SAT complex (B): (A) the spectra at 10.4, 20.4, 30.4, 40.4, and 60.4 ms after the start of the reaction, $[H_2tpp]_o = 1.5 \times 10^{-6}$ mol dm$^{-3}$, $[Cu^{2+}] = 5.47 \times 10^{-4}$ mol dm$^{-3}$, and 25.0°C; (B) the peaks of the N–H (higher field) and $\beta$-pyrrole protons (lower field) for $H_2$tpp (upper, $4.0 \times 10^{-2}$ mol dm$^{-3}$ of $H_2$tpp in $CDCl_3$) and the SAT complex (lower, $CD_3CN$ solution containing $7.0 \times 10^{-3}$ mol dm$^{-3}$ of $H_2$tpp and $3.5 \times 10^{-2}$ mol dm$^{-3}$ of $Cu^{2+}$) (adopted from Ref. 36 with permission).

coordinated to the Cu(II) ion, respectively. A similar splitting was reported for $H_2$tpp at the low temperature of –80°C, because the N–H tautomerism at such a low temperature was frozen,[69,70] where the signal of the $\beta$-pyrrole protons of the pyrrole groups with N–H protons was observed at a lower field relative to that of the pyrrolenine groups without the N–H protons. The opposite trend in chemical shift was observed for the SAT complex, *i.e.*, the doublet peak assigned to the $\beta$-pyrrole protons appears at a higher field (see Fig. 4B). This indicates that the two pyrrolenine nitrogens without an NH proton bind to the paramagnetic Cu(II) ion, because the dipole-dipole and scalar coupling interactions with the paramagnetic ion lead to their downfield shift. Furthermore, the peak for NH protons was shifted downfield relative to that of $H_2$tpp. This is ascribed to both the distortion of the porphyrin ring and the dipole–dipole interaction with the paramagnetic copper(II) ion. Because the NH protons in $H_2$tpp are highly shifted to the upper field due to the ring current of the planar porphyrin ring, the distortion of the porphyrin ring in the SAT complex then leads to the downfield shift.

Two types of porphyrin skeletons (**1** and **2** in Scheme 2) are possible for the SAT complex with the pyrrolenine nitrogens coordinating to the Cu(II) ion. The observed $^1$H NMR spectrum determines the symmetrical structure of **1**, because, in the case of **2**, the two $\beta$-pyrrole protons of the pyrrolenine ring are not identical.

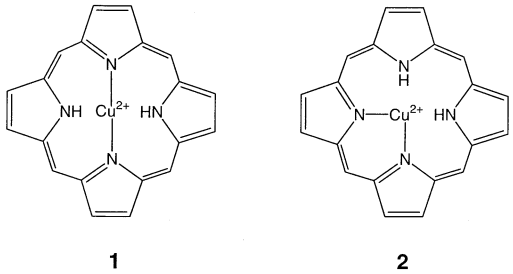


Scheme 2

Table 4 Structure parameters around the $Cu^{2+}$ ion as determined by fluorescent EXAFS[a]

| Complex | Interaction | *N* | *R*/Å |
|---|---|---|---|
| $Cu(H_2tpp)(an)_4^{2+}$ | Cu–N(pyr)[b] | 1.6 | 2.05 |
| | $Cu–N(an)_{eq}$[c,d] | 2.4 | 1.98 |
| | $Cu–N(an)_{ax}$[c,e] | 2.4 | 2.32 |
| Cu(tpp) | Cu–N(pyr)[b] | 4[f] | 2.02 |
| Cu(tpp)[g] | Cu–N(pyr)[b] | 4 | 1.98 – 2.01 |
| $Cu(an)_6^{2+}$ | $Cu–N(an)_{eq}$[c,d] | 4[f] | 1.99 |
| | $Cu–N(an)_{ax}$[c,e] | 2[f] | 2.40 |
| $Cu(an)_6^{2+}$[h] | $Cu–N(an)_{eq}$[c,e] | 4[f] | 1.99 |
| | $Cu–N(an)_{ax}$[c,e] | 2[f] | 2.23 |

a. Errors of *N* and *R* are estimated to be *ca.* 0.2 and 0.01 Å respectively.
b. Interaction between Cu and pyrrolenine nitrogen.
c. Interaction between Cu and nitrogen of bound AN.
d. Equatorial site of the Cu(II) ion.
e. Axial site of the Cu(II) ion.
f. Fixed during the least-squares calculation.
g. In single crystal, Ref. 71 – 74.
h. Determined by EXAFS measurement in transmission mode, Ref. 75.

### 5·2 Structure of Cu(II)-SAT complex as determined by fluorescent EXAFS

The structure parameters around $Cu^{2+}$ in the Cu(II)-SAT complex were determined by a fluorescent EXAFS method and are tabulated in Table 4.[37]

For the Cu(II)-SAT complex, the observed EXAFS data are satisfactorily reproduced by three kinds of Cu–N interactions with *N* values of *ca.* 2, *i.e.*, the Cu–N(pyr), $Cu–N(an)_{eq}$, and $Cu–N(an)_{ax}$ interactions with the *N* and *R* values of 1.6 and 2.05 Å, 2.4 and 1.98 Å, and 2.4 and 2.32 Å, respectively, where N(pyr), $N(an)_{eq}$, and $N(an)_{ax}$, respectively, denote the coordinating nitrogen atom of $H_2$tpp, AN at the equatorial site, and AN at the axial site. Interestingly, the *R* value for Cu–N(pyr) in the Cu(II)-SAT complex ($Cu(H_2tpp)(an)_4^{2+}$) is larger than that (2.02 Å) of Cu(tpp),[71–74] while the *R* value of 1.98 Å for $Cu–N(an)_{eq}$ is alomost identical with that (1.99 Å) of the equatorial site of $Cu(an)_6^{2+}$.[75] The longer bond distance of Cu–N(pyr) rather than that of Cu(tpp), in which the $Cu^{2+}$ ion is just incorporated into the porphyrin core, is ascribed to the limitation due to the steric geometry of the porphyrin core. Consequently, the bite angle of N(pyr)–Cu–N(pyr) should be much greater than 90°, considering the bidentate coordination of the opposite two pyrrolenine groups of $H_2$tpp in the Cu(II)-SAT complex, as indicated by the $^1$H NMR spectrum (see 5·1).

It is well-known that, by steric restriction of bound ligands, the geometry around the $Cu^{2+}$ ion is easily varied with a variety

of dihedral angles between the two N–Cu–N planes of the equatorial site from 0 to 90°.[76-78] However, the EXAFS spectrum of the Cu(II)-SAT complex was satisfactorily reproduced by the model with an axial Cu–N(an) interaction, and the result is in agreement with that observed for the structure parameters around the $Cu^{2+}$ ion in the Cu(II)/Hg(II) heterodinuclear porphyrin intermediate (see 4·2).[66] Furthermore, the fact that the *R* value of Cu–$N(an)_{eq}$ is almost the same as that of $Cu(an)_6^{2+}$ strongly indicates that the AN molecules coordinate to the $Cu^{2+}$ ion at the equatorial sites in the distorted octahedral environment because the bond distance in the tetrahedral analogue with a reduced coodination number should be shortened, as indicated by the structural data of the solvated metal ions with a reduced solvation number in bulky solvents.[59,79,80] Thus, we can conclude that the dihedral angle between the two N–Cu–N planes of the equatorial site around the $Cu^{2+}$ ion in the Cu(II)-SAT complex may be *ca*. 0°. Therefore, the Cu(II)-SAT complex seems to have an axially elongated and equatorially distorted six-coordinate geometry.

### 5·3 Mechanism of SAT complex formation

Furthermore, we followed the formation rate of the TPP-SAT complexes of metal(II) ions (M(II) = $Mn^{2+}$, $Fe^{2+}$, $Co^{2+}$, $Ni^{2+}$, and $Zn^{2+}$) as well as $Cu^{2+}$ in AN using the stopped-flow technique.[37] In Fig. 5 is visualized the trend in variation of the rate constant, $k_f$, of the TPP-SAT complex formation in AN for a series of $M^{2+}$ ions and in the rate constant, $k_{ex}$, of the solvent exchange in $H_2O$,[81-85] methanol,[86-88] DMF,[88-91] and AN.[88,92-95] Although the values of $k_{ex}$ for the solvent exchange on the $Cu^{2+}$ and $Zn^{2+}$ ions in AN are not available, the variation in $k_{ex}$ for a series of $M^{2+}$ ions is similar for various solvents, as expected from Fig. 5. Therefore, the observed variation trends in $k_f$ are regarded as being similar to that in $k_{ex}$ for a series of $M^{2+}$ ions. This characteristic strongly indicates that the rate-determining step for the SAT complex formation is similar to that of the solvent exchange; *i.e*., the rate-determining step of the SAT complex formation is the bond rupture between the $M^{2+}$ ion and a bound AN molecule simultaneously accompanying the bond formation between the $M^{2+}$ ion and the first pyrrolenine nitrogen of $H_2$tpp. The chelate ring closure to form the SAT complex, in which $H_2$tpp is bound to $M^{2+}$ as a bidentate ligand according to the EXAFS and $^1$H NMR results, must be faster than the rate-determining exchange. The values of $k_f$ are, however, 4 – 6 orders of magnitude smaller than the $k_{ex}$ values, and thus, it can be expected that there is a large energetic loss due to the fast preequilibria prior to the rate-determining step. If the rapid deformation equilibrium ($K_D$) of the porphyrin ring and the rapid outer-sphere encounter formation equilibrium ($K_{os}$) between the AN-solvated $M^{2+}$ ion and the deformed porphyrin ($H_2$*tpp*) are assumed to precede the rate-determining exchange (reaction (17)) between the bound nitrogen of the AN molecule and the first pyrrolenine nitrogen of $H_2$tpp, as shown by the equations:

$$H_2tpp \overset{K_D}{\rightleftharpoons} H_2tpp \quad (15)$$

$$M(an)_6^{2+} + H_2tpp \overset{K_{os}}{\rightleftharpoons} M(an)_6^{2+}\cdots H_2tpp \quad (16)$$

$$M(an)_6^{2+}\cdots H_2tpp \overset{K_{SAT}}{\rightleftharpoons} M(an)_5(H_2tpp)^{2+} + AN \quad (17)$$

and

$$M(an)_5(H_2tpp)^{2+} \overset{fast}{\rightleftharpoons} M(an)_4(H_2tpp)^{2+} + AN \quad (18)$$

then $k_f$ for the formation of the SAT complex ($M(an)_4(H_2tpp)^{2+}$) is expressed by

$$k_f = K_D K_{os} k_{SAT}. \quad (19)$$

Because the values of $k_f$ for a series of $M^{2+}$ ions are parallel to the $k_{ex}$ values, the $k_{SAT}$ term in Eq. (19) may be approximately replaced by $k_{ex}$ in AN. Although the large deformation of the $\pi$-electron-conjugated system is unfavorable in enthalpy, it may be effectively compensated in entropy, since significant amounts of freedom in the intramolecular vibration and rotation modes may appear due to the $C_{2v}$ deformation of the porphyrin core.

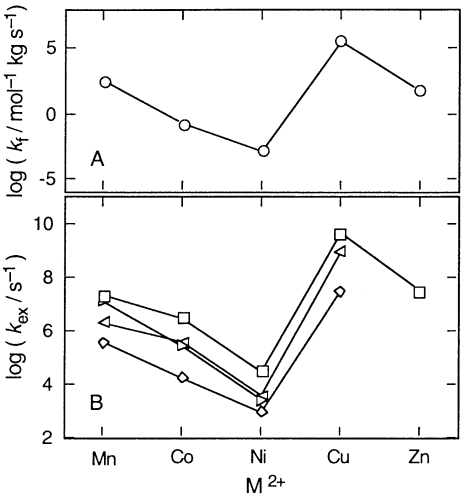


Fig. 5 Formation rate constants of the SAT complexes in acetonitrile (A) and solvent exchange rate constants (B). In part B, the values in $H_2O$, methanol, *N*,*N*-dimethylformamide, and acetonitrile are given by squares, diamonds, left-pointed triangles, and right-pointed triangles, respectively (adopted from Ref. 37 with permission).

## 6 Rates for Deprotonation of SAT Complex

### 6·1 Deprotonation of SAT complex by Brønsted bases leading to metalloporphyrin

Figure 6 shows the spectral change with clear isosbestic points at 411, 430, 524, and 553 nm for deprotonation of the Cu(II)-SAT complex with 3-methylpyridine (mpy) in AN.[38] The increasing absorbance at 414 and 540 nm, which are characteristic for the Cu(tpp) complex, means that the pyrrole protons are dissociated from the Cu(II)-SAT complex by the reaction with the mpy base. The deprotonation rate is first order with respect to the mpy base in the [mpy] range lower than $8 \times 10^{-3}$ mol dm$^{-3}$. The first deprotonation means that the free mpy as the proton acceptor directly attacks the first pyrrole proton in the Cu(II)-SAT complex ($Cu(H_2tpp)^{2+}$).

$$Cu(H_2tpp)^{2+} + mpy \overset{k_1}{\rightleftharpoons} Cu(Htpp)^{+} + Hmpy^{+}$$

Because two pyrrole protons are dissociated from the Cu(II)-SAT complex leading to Cu(tpp), the deprotonation may be expected to occur in two steps according to Eqs. (20) and (21). The absorbance change at 414 nm as a function of reaction time was perfectly reproduced by a single exponential function in a large excess of base.

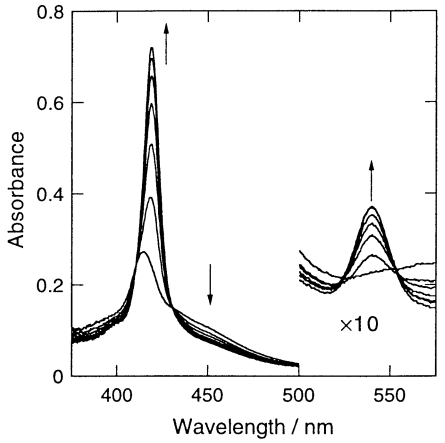


Fig. 6 Absorption spectral change for the deprotonation reaction of the Cu(II)-SAT complex with 3-methylpyridine. $C_{Cu(II)\text{-}SAT} = 3.2 \times 10^{-6}$ mol dm$^{-3}$ and $C_{mpy} = 4.27 \times 10^{-3}$ mol dm$^{-3}$. The spectra at 0, 77, 154, 231, 308, 385, and 462 ms after the mixing of sample solutions were depicted.

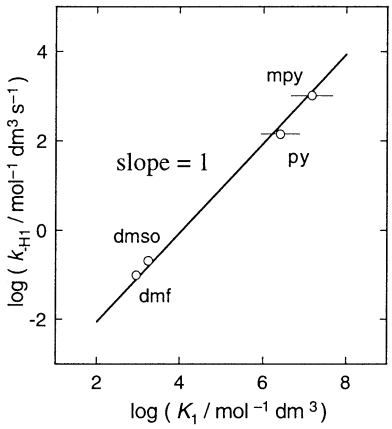


Fig. 7 Relation between $\log(k_1/\text{mol}^{-1}\ \text{dm}^3\ \text{s}^{-1})$ and $\log(K_1/\text{mol}^{-1}\ \text{dm}^3)$ for a series of Brønsted bases. The slope of the straight line is unity.

$$Cu(H_2tpp)^{2+} + B \underset{}{\overset{k_{-H1}}{\rightleftharpoons}} Cu(Htpp)^{+} + HB^{+} \quad (20)$$

$$Cu(Htpp)^{+} + B \rightleftharpoons Cu(tpp)^{+} + HB^{+} \quad (21)$$

If the second deprotonation is a rate-determining step with fast equilibration of the first deprotonation, the absorbance change should not be reproduced by the single exponential function, because the $HB^+$ concentation changes during the reaction. The first deprotonation is thus concluded to be rate-determining and the second is much faster.

### 6·2 Deprotonation mechansim of SAT complex

In Fig. 7 are plotted the rate constants, $k_1$, for the deprotonation of the Cu(II)-SAT complex with a series of Brønsted bases (mpy, py, dmso, and dmf) *versus* the formation constants, $K_1$, for the mono Cu(II) complex in AN.[38] The linear relation with the slope of unity between log $k_1$ and log $K_1$ strongly indicates that the Brønsted base as nucleophile attacks a pyrrole proton in the Cu(II)-SAT complex. Therefore, the stronger the $\sigma$ donecity of the Brønsted base, the stabler the interaction between the pyrrole proton and the donating atom of the base becomes during the transition state of the deprotonation. The base should attack the proton on the pyrrole nitrogen in the SAT complex ($k_{-H1}$ path) and the second deprotonation is fast.

## 7 General Metalation Mechanism

### 7·1 Metalloporphyrin formation mechanism in coordinating solvents

In this final stage, we can generally describe the mechanisms of metalloporphyrin formation on the basis of the present crucial results obtained in AN, together with the previously reported results for a variety of metal ions and porphyrins. The resolvable elementary reactions during the metalation processes of a general porphyrin ($H_2$por) with a fully solvated divalent metal ion ($MS^*_n{}^{2+}$) in a common donating solvent (S) as a base are completely expressed by the following several processes: the distortion of the porphyrin ring (Eq. (22)) where $H_2$*por* is a deformed porphyrin, the outer-sphere encounter formation (Eq. (23)), the exchange of a bound solvent molecule with the first pyrrolenine nitrogen (Eq. (24)), the chelate ring closure to form the SAT complex (Eq. (25)), the first deprotonation of the pyrrole nitrogen in the SAT complex (Eq. (26)), and the second deprotonation to form a metalloporphyrin (Eq. (27)).

$$H_2por \underset{k_{-D}}{\overset{k_D}{\rightleftharpoons}} H_2por,\ K_D = \frac{k_D}{k_{-D}} \quad (22)$$

$$MS^*_n{}^{2+} + H_2por \underset{k_{-OS}}{\overset{k_{OS}}{\rightleftharpoons}} MS^*_n{}^{2+}\cdots H_2por,\ K_{os} = \frac{k_{OS}}{k_{-OS}} \quad (23)$$

$$MS^*_n{}^{2+}\cdots H_2por \underset{k_{-SAT}}{\overset{k_{SAT}}{\rightleftharpoons}} MS^*_{n-1}(H_2por)^{2+} + S^* \quad (24)$$

$$MS^*_{n-1}(H_2por)^{2+} \underset{k_{-RC}}{\overset{k_{RC}}{\rightleftharpoons}} MS^*_{n-2}(H_2por)^{2+} + S^*,\ K_R = \frac{k_{RC}}{k_{-RC}} \quad (25)$$

$$MS^*_{n-2}(H_2por)^{2+} + S \underset{k_{H1}}{\overset{k_{-H1}}{\rightleftharpoons}} MS^*_{n-3}(Hpor)^{+} + HS^{+} + S^*,$$

$$K_{-H1} = \frac{k_{-H1}}{k_{H1}} \quad (26)$$

$$MS^*_{n-3}(Hpor)^{+} + S \underset{k_{H2}}{\overset{k_{-H2}}{\rightleftharpoons}} M(por) + HS^{+} + (n-3)S^*,$$

$$K_{-H2} = \frac{k_{-H2}}{k_{H2}} \quad (27)$$

where S* and S are a coordinating solvent molecule and a solvent molecule in the bulk, respectively. The value of $k_D$ is reported to be $4.6 \times 10^7$ s$^{-1}$ at 25°C for 5,10,15,20-tetrakis(4-*N*-methylpyridyl)porphyrin in water,[96] and the pathway of $k_{os}$ is considered to be diffusion-controlled. Furthermore, the $k_{RC}$ step for the chelate ring closure is generally considered to be faster than the coordination of a first donor atom ($k_{SAT}$). The present results indicate that the $k_{SAT}$ path is a rate-determining step for the metalation process in the presence of the base as a proton acceptor.

### 7·2 Conclusions

In conclusion, we can generally describe the metalation mechanism as shown in Fig. 8. According to reactions (22) – (27), the forward and backward rates for reaction (1) ($R_f$ and $R_b$) are described by Eqs. (28) and (29), respectively.

$$R_f = K_D K_{OS} k_{SAT}[MS_6{}^{2+}][H_2por] \quad (28)$$

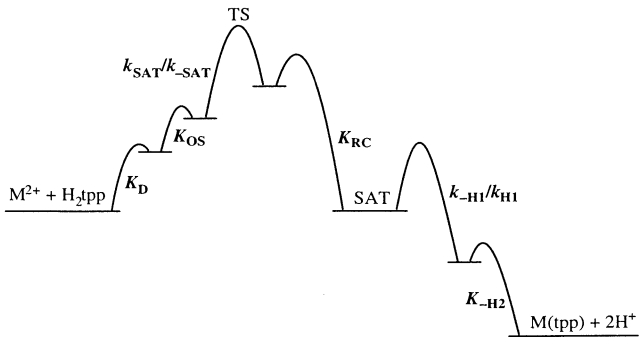


Fig. 8 Schematic energy profile of the overall metalation reaction of $H_2$tpp.

$$R_b = K_{-H2}^{-1}K_{-H1}^{-1}K_{RC}^{-1}k_{-SAT}[HS^+]^2[M(por)] \quad (29)$$

These expressions for the metalation and demetalation rates can explain some previously observed trends as follows: (1) the parallel dependence of the metalation rate on the solvent exchange rate and the lability of a bound solvent due to the $k_{SAT}$ step;[23-25,29,97-100] (2) the acceleration of the metalation rate for the nonplanar porphyrins due to the $K_D$ step;[8,24,28-30,43,56,96,101,102] (3) the dependence of the metalation rate on the Brønsted basicity of porphyrins due to the $k_{SAT}$ step;[30,103,104] (4) the $[H^+]^2$-dependent rate law for the demetalation due to the $K_{H1}$ and $K_{H2}$ steps;[105-107] (5) the dependence of the metalation rate of the charged porphyrins on the ionic strength due to the $K_{os}$ step.[108] The formation and deprotonation kinetics of the SAT complex, obtained by the strategic use of AN as a solvent with very weak basicity, have been independently demonstrated in this study, and we have unified the reaction scheme for the overall metalation of the porphyrin.

## 8 Acknowledgements

The authors sincerely thank all the co-workers and students whose names appear in the references and who devoted themselves to the present study. The financial support by the Grants-in-Aid for Scientific Research (Nos. 11354009, 11554030, and 12874094) from the Ministry of Education, Science, Sports, and Culture of Japan is gratefully acknowledged.

## 9 References

1. M. Tabata and M. Tanaka, *Anal. Lett*., **1980**, *13*, 149.
2. H. Ishii, H. Koh, and K. Satoh, *Anal. Chim. Acta*, **1982**, *136*, 347.
3. H. Ishii, Y. Satoh, and K. Satoh, *Anal. Sci*., **1989**, *5*, 713.
4. K. Endo and S. Igarashi, *Bull. Chem. Soc. Jpn*., **1995**, *68*, 3085.
5. S. Igarashi, T. Aihara, and T. Yotsuyanagi, *Anal. Chim. Acta*, **1996**, *323*, 63.
6. M. Inamo, A. Tomita, Y. Inagaki, N. Asano, K. Suenaga, M. Tabata, and S. Funahashi, *Inorg. Chim. Acta*, **1997**, *256*, 77.
7. M. Tabata, J. Nishimoto, and K. Kusano, *Talanta*, **1998**, *46*, 703.
8. S. Funahashi, Y. Ito, H. Kakito, M. Inamo, Y. Hamada, and M. Tanaka, *Mikrochim. Acta* [Wien], **1986 I**, 33.
9. M. Tabata and M. Tanaka, *Tr. Anal. Chem*., **1991**, *10*, 128.
10. S. Taketani and R. Tokunaga, *J. Biol. Chem*., **1981**, *256*, 12748.
11. H. A. Dailey, *J. Biol. Chem*., **1982**, *257*, 14714.
12. H. A. Dailey and J. E. Fleming, *J. Biol. Chem*., **1983**, *258*, 11453.
13. H. A. Dailey, *J. Biol. Chem*., **1984**, *259*, 2711.
14. H. A. Dailey, *Biochemistry*, **1985**, *24*, 1287.
15. H. A. Dailey and J. E. Fleming, *J. Biol. Chem*., **1986**, *261*, 7902.
16. H. A, Dailey, C. S. Jones, and S. W. Karr, *Biochim. Biophys. Acta*, **1989**, *999*, 7.
17. D. K. Lavallee, "*The Chemistry and Biochemistry of N-Substituted Porphyrins*", **1987**, VCH, New York.
18. D. K. Lavallee, *Mol. Struct. Energ*., **1988**, *9*, 279.
19. H. A. Dailey, "*Biosynthesis of Heme and Chlorophylls*", **1990**, McGraw-Hill, New York.
20. S. Taketani, "*Regulation of Heme Protein Synthesis*", ed. H. Fujita, **1994**, AlphaMed Press, Ohio.
21. J. W. Buchler, "*Porphyrins and Metalloporphyrins*", ed. K. M. Smith, **1975**, Elsevier, Amsterdam.
22. D. Dolphin, "*The Porphyrins*", **1978**, Vol. VI – VII, Academic Press, New York.
23. P. Hambright and P. B. Chock, *J. Am. Chem. Soc*., **1974**, *96*, 3123.
24. M. J. B.-Ackerman and D. K. Lavallee, *Inorg. Chem*., **1979**, *18*, 3358.
25. J. Turay and P. Hambright, *Inorg. Chem*., **1980**, *19*, 562.
26. S. Funahashi, K. Saito, and M. Tanaka, *Bull. Chem. Soc. Jpn*., **1981**, *54*, 2695.
27. R. F. Pasternack, G. C. Vogel, C. A. Skowronek, R. K. Harris, and J. G. Miller, *Inorg. Chem*., **1981**, *20*, 3763.
28. S. Funahashi, Y. Yamaguchi, and M. Tanaka, *Bull. Chem. Soc. Jpn*., **1984**, *57*, 204.
29. S. Funahashi, Y. Yamaguchi, and M. Tanaka, *Inorg. Chem*., **1984**, *23*, 2249.
30. L. R. Robinson and P. Hambright, *Inorg. Chim. Acta*, **1991**, *185*, 17.
31. E. B. Fleischer and J. H. Wang, *J. Am. Chem. Soc*., **1960**, *82*, 3498.
32. B. F. Burnham and J. J. Zuckerman, *J. Am. Chem. Soc*., **1970**, *92*, 1547.
33. J. P. Macquet and T. Theophanides, *Can. J. Chem*., **1973**, *51*, 219.
34. K. Letts and R. A. Mackay, *Inorg. Chem*., **1975**, *14*, 2993.
35. E. B. Fleischer and F. Dixon, *Bioinorg. Chem*., **1977**, *7*, 129.
36. Y. Inada, Y. Sugimoto, Y. Nakano, Y. Itoh, and S. Funahashi, *Inorg. Chem*., **1998**, *37*, 5519.
37. Y. Inada, Y. Nakano, M. Inamo, M. Nomura, and S. Funahashi, *Inorg. Chem*., **2000**, *39*, 4793.
38. Y. Inada, T. Yamaguchi, H. Satoh, and S. Funahashi, *Inorg. React. Mech*., **2000**, *2*, 277.
39. R. B. Jordan, "*Reaction Mechanisms of Inorganic and Organometallic Systems*", **1991**, Oxford, New York.
40. M. L. Tobe and J. Burgess, "*Inorganic Reaction Mechanisms*", **1999**, Longman, New York.
41. K. Ishihara, S. Funahashi, and M. Tanaka, *Inorg. Chem*., **1983**, *22*, 2564.
42. S. Aizawa, Y, Tsuda, Y. Ito, K. Hatano, and S. Funahashi, *Inorg. Chem*., **1993**, *32*, 1119.
43. B. Shah, B. Shears, and P. Hambright, *Inorg. Chem*., **1971**, *10*, 1828.
44. D. E. Goldberg and K. M. Thomas, *J. Am. Chem. Soc*., **1976**, *98*, 913.

45. O. P. Anderson and D. K. Lavallee, *J. Am. Chem. Soc*., **1976**, *98*, 4670.
46. O. P. Anderson and D. K. Lavallee, *J. Am. Chem. Soc*., **1977**, *99*, 1404.
47. O. P. Anderson and D. K. Lavallee, *Inorg. Chem*., **1977**, *16*, 1634.
48. D. K. Lavallee, A. B. Kopelove, and O. P. Anderson, *J. Am. Chem. Soc*., **1978**, *100*, 3025.
49. O. P. Anderson, A. B. Kopelove, and D. K. Lavallee, *Inorg. Chem*., **1980**, *19*, 2101.
50. D. Kuila and D. K. Lavallee, *J. Am. Chem. Soc*., **1984**, *106*, 448.
51. D. K. Lavallee, A. Wite, A. Diaz, J.-P. Battioni, and D. Mansuy, *Tetrahedron Lett*., **1986**, *27*, 3521.
52. C. K. Schauer, O. P. Anderson, D. K. Lavallee, J.-P. Battioni, and D. Mansuy, *J. Am. Chem. Soc*., **1987**, *109*, 3922.
53. A. L. Balch, C. R. Cornman, L. Latos-Grazynski, and M. M. Olmstead, *J. Am. Chem*. Soc., **1990**, *112*, 7552.
54. G. M. McLaughlin, *J. Chem. Soc., Perkin Trans*., **1974**, *2*, 136.
55. T. J. Bartczak, L. Latos-Grazynski, and A. Wyslouch, *Inorg. Chim. Acta*, **1990**, *171*, 205.
56. Y. Shimizu, K. Taniguchi, Y. Inada, S. Funahashi, Y. Tsuda, Y. Ito, M. Inamo, and M. Tanaka, *Bull. Chem. Soc. Jpn*., **1992**, *65*, 771.
57. D. K. Lavallee and O. P. Anderson, *J. Am. Chem. Soc*., **1982**, *104*, 4707.
58. S. Funahashi, Y. Yamaguchi, K. Ishihara, and M. Tanaka, *J. Chem. Soc., Chem. Commun*., **1982**, 976.
59. Y. Inada, K. Sugimoto, K. Ozutsumi, and S. Funahashi, *Inorg. Chem*., **1994**, *33*, 187.
60. M. Tabata and M. Tanaka, *J. Chem. Soc., Chem. Commun*., **1985**, 42.
61. Y. Ducommun, G. Laurenczy, and A. E. Merbach, *Inorg. Chem*., **1988**, *27*, 1148.
62. M. Tabata and W. Miyata, *Chem. Lett*., **1991**, 785.
63. L. R. Robinson and P. Hambright, *Inorg. Chem*., **1992**, *31*, 652.
64. Y. Inada, S. Funahashi, and H. Ohtaki, *Rev. Sci. Instum*., **1994**, *65*, 18.
65. Y. Inada and S. Funahashi, *Recent Res. Devel. Pure Appl. Chem*., **1998**, *2*, 347.
66. H. Ohtaki, Y. Inada, S. Funahashi, M. Tabata, K. Ozutsumi, and K. Nakajima, *J. Chem. Soc., Chem. Commun*., **1994**, 1023.
67. Y. Inada, K. Ozutsumi, S. Funahashi, S. Soyama, T. Kawashima, and M. Tanaka, *Inorg. Chem*., **1993**, *32*, 3010.
68. M. Tabata and K. Ozutsumi, *Bull. Chem. Soc. Jpn*., **1992**, *65*, 1438.
69. C. B. Storm and Y. Teklu, *J. Am. Chem. Soc*., **1972**, *94*, 1745.
70. C. B. Storm, Y. Teklu, and A. Sokoloski, *Ann. N. Y. Acad. Sci*., **1973**, *206*, 631.
71. M. P. Bryn, C. J. Curtis, Y. Hsiou, S. I. Khan, P. A. Sawin, S. K. Tendick, A. Terzis, and C. E. Strouse, *J. Am. Chem. Soc*., **1993**, *115*, 9480.
72. M. P. Bryn, C. J. Curtis, I. Goldberg, Y. Hsiou, S. I. Khan, P. A. Sawin, S. K. Tendick, A. Terzis, and C. E. Strouse, *J. Am. Chem. Soc*., **1991**, *113*, 6549.
73. B. S. Erler, W. F. Scholz, Y. J. Lee, W. R. Scheidt, and C. A. Reed, *J. Am. Chem. Soc*., **1987**, *109*, 2644.
74. E. B. Fleischer, C. K. Miller, and L. E. Webb, *J. Am. Chem. Soc*., **1964**, *86*, 2342.
75. S. Funahashi and Y. Inada, *Tr. Inorg. Chem*., **1998**, *5*, 15.
76. M. T. Miller, P. K. Gantzel, and T. B. Karpishin, *Inorg. Chem*., **1998**, *37*, 2285.
77. E. Müler, G. Bernardinelli, and J. Reedijk, *Inorg. Chem*., **1996**, *35* ,1952.
78. H. Adams, N. A. Bailey, D. E. Fenton, S. Moss, and C. O. Rodriguez de Barbarin, *J. Chem. Soc., Dalton Trans*., **1986**, 693.
79. Y. Inada, H. Hayashi, K. Sugimoto, and S. Funahashi, *J. Phys. Chem. A*, **1999**, *103*, 1401.
80. K. Ozutsumi, Y. Abe, R. Takahashi, and S. Ishiguro, *J. Phys. Chem*., **1994**, *98*, 9894.
81. Y. Ducommon, K. E. Newman, and A. E. Merbach, *Helv. Chim. Acta*, **1979**, *62*, 2511.
82. Y. Ducommun, K. E. Newman, and A. E. Merbach, *Inorg. Chem*., **1980**, *19*, 3696.
83. P. E. Hoggard, H. W. Dodgen, and J. P. Hunt, *Inorg. Chem*., **1971**, *10*, 959.
84. D. H. Powell, L. Helm, and A. E. Merbach, *J. Chem. Phys*., **1991**, *95*, 9258.
85. F. Fittipaldi and S. Petrucci, *J. Phys. Chem*., **1967**, *71*, 3414.
86. F. K. Meyer, K. E. Newman, and A. E. Merbach, *J. Am. Chem. Soc*., **1979**, *101*, 5588.
87. L. Helm, S. F. Lincoln, A. E. Merbach, and D. Zbinden, *Inorg. Chem*., **1986**, *25*, 2550.
88. F. K. Meyer, K. E. Newman, and A. E. Merbach, *Inorg. Chem*., **1979**, *18*, 2142.
89. T.-M. Chen and L. O. Morgan, *J. Phys. Chem*., **1972**, *76*, 1973.
90. S. Funahashi and R. B. Jordan, *Inorg. Chem*., **1977**, *16*, 1301.
91. D. H. Powell, P. Furrer, P.-A. Pittet, and A. E. Merbach, *J. Phys. Chem*., **1995**, *99*, 16622.
92. Y. Inada, T. Sugata, K. Ozutsumi, and S. Funahashi, *Inorg. Chem*., **1998**, *37*, 1886.
93. M. J. Sisley, Y. Yano, and T. W. Swaddle, *Inorg. Chem*., **1982**, *21*, 1141.
94. Y. Yano, M. T. Fairhurst, and T. W. Swaddle, *Inorg. Chem*., **1980**, *19*, 3267.
95. A. Monnerat, P. Moore, K. E. Newman, and A. E. Merbach, *Inorg. Chim. Acta*, **1981**, *47*, 139.
96. R. F. Pasternack, N. Sutin, and D. H. Turner, *J. Am. Chem. Soc*., **1976**, *98*, 1908.
97. E. I. Choi and E. B. Fleischer, *Inorg. Chem*., **1963**, *2*, 94.
98. E. B. Fleischer, E. I. Choi, P. Hambright, and A. Stone, *Inorg. Chem*., **1964**, *3*, 1284.
99. D. J. Kingham and D. A. Brisbin, *Inorg. Chem*., **1970**, *9*, 2034.
100. M. Tabata and M. Tanaka, *Inorg. Chem*., **1988**, *27*, 203.
101. D. K. Lavallee, "*The Chemistry and Biochemistry of N-Substituted Porphyrins*", **1987**, VCH, New York.
102. S. Aizawa, Y. Tsuda, Y. Ito, K. Hatano, and S. Funahashi, *Inorg. Chem*., **1993**, *32*, 1119.
103. J. B. Reid and P. Hambright, *Inorg. Chem*., **1977**, *16*, 968.
104. A. Shamim and P. Hambright, *Inorg. Chem*., **1980**, *19*, 564.
105. B. Shears, B. Shah, and P. Hambright, *J. Am. Chem. Soc*., **1971**, *93*, 776.
106. R. Rahimi, T. P. G. Sutter, and P. Hambright, *J. Coord. Chem*., **1995**, *34*, 283.
107. M. Tabata, K. Oshita, and M. Tanaka, *Mikrochim. Acta*, [Wien], **1985 I**, 397.
108. J. Nwaeme and P. Hambright, *Inorg. Chem*., **1984**, *23*, 1990.